Experimental reproduction of an extreme sea state in two wave tanks at various generation scales

Maxime Canard, Guillaume Ducrozet, Benjamin Bouscasse

Experimental reproduction of an extreme sea state in two wave tanks at various generation scales.

1st Maxime Canard
LHEEA
Ecole Centrale Nantes
Nantes, France
maxime.canard@ec-nantes.fr

2nd Guillaume Ducrozet
LHEEA
Ecole Centrale Nantes
Nantes, France
guillaume.ducrozet@ec-nantes.fr

3rd Benjamin Bouscasse
LHEEA
Ecole Centrale Nantes
Nantes, France
benjamin.bouscasse@ec-nantes.fr

OCEANS 2022 - Chennai | 978-1-6654-1821-8/22/$31.00 ©2022 IEEE | DOI: 10.1109/OCEANSChennai45887.2022.9775216

***Abstract*—**
Wave structure interaction experiments require the generation of design sea states at model scale in wave tank environments. A vast majority of the industrial practices rely on the stochastic approach. Long free surface elevation time-series (realizations) are generated by the wave maker of the tank. The input signals are built in the Fourier space, based on a design wave spectrum and random phases. The number of realizations is large enough to contain the events leading to the extreme responses. The quality of the wave field is checked at the structure position (target position). The two main quantities of interest are i) the wave spectrum and ii) the crest height distribution (characterizing the occurrence of the extreme events). As the wave propagation is not linear, those quantities vary from the wavemaker to the target position. To correct the spectrum, existing wave generation procedures iterate on the wavemaker motion. Using such a procedure, the present experimental study focused on the accurate reproduction of an extreme unidirectional design sea state. The later induced numerous and strong breaking events. It was generated in two tanks at two different model scales, at the same target position. The wave height statistics varied from one configuration to an other. The induced limitations for the industrial practices were studied. A particular attention was paid to the effects of the generation scale on the breaking events.

***Index Terms*—Wave Tank, Extreme Sea State, Breaking waves, Ocean Engineering**

I. Introduction

To assess the reliability either of a ship or an offshore structure, sea keeping studies are performed at model scale in numerical or experimental wave tanks. The wave conditions for such tests are defined by classification societies [1]. They establish a set of design sea states that the structure should be able to withstand.

A design sea state $S_{\text{design}}(f)$ (with f the frequency) is characterised by a wave energy spectrum and a certain duration. The later is usually 3hours at full scale (which corresponds to 10 to 30min at model scale). This duration is associated with a short-term probability P_{design} which is the probability of occurrence of the most extreme events to consider. As an example, for a peak period at full scale $T_p = 15.5s$ (which is the period of the sea state studied in the present paper), approximately 700 waves occur within 3hours. Then, the wave structure interaction test should take into account the most extreme events that occur every 700 waves, at a probability $P_{\text{design}} = 1/700 = 1.4\ 10^{-3}$.

To generate a sea state, most of the industrial methods use a stochastic approach. Several long free surface elevation time-series (realizations) are generated by the wave maker, at the beginning of the tank. The input signals are built in the Fourier space, based on the design spectrum and random phases [2]. The number and the length of the realizations is large enough to ensure that the quantities of interest are statistically reliable up to P_{design}. Note that this corresponds to a larger number of waves than $1/P_{\text{design}}$.

The qualification of the generated wave field is performed at a target position X_t (usually the position of the tested structure). It mainly relies on two stochastic quantities [1], [3]. The first one is the mean wave spectrum (over all the realizations). It is compared to the design spectrum. The second one is the ensemble crest height distribution (accounting for all the realizations). The later corresponds to the probability of exceedance of the zero-crossing crest height (an event being here defined by the crest heigth of a zero-crossing wave). The crest distribution has to be statistically reliable up to P_{design}.

However, nonlinear phenomena affect the propagation of the waves. Therefore, even if the design sea state is accurately generated at the wavemaker position, the control of the wave field at the target position is not straightforward [4], [5].

It is then important to understand how the quantities of interest are affected by the wave propagation. Note that the scope of this study is limited to irregular unidirectional waves. At first, for nonlinear wave conditions, high order nonlinear interactions such as modulational instability and near-resonant interactions occur [6]. As a consequence, i) the spectrum width gets larger and ii) the probability of the extreme events (i. e. events with large crest height) increases as the waves propagate. This as been studied theoretically in [7], [8] and experimentally in [9]–[14]. Those phenomena are directly dependent on the steepness and the width of the input wave spectrum. Moreover, for highly steep wave conditions, breaking events occur. They dissipate energy and affect the shape of the waves. As a result, the significant wave height

978-1-6654-1821-8/22/$31.00 ©2022 IEEE

H_s decreases along the tank and the spectrum shape is affected [9], [15], [16].

To counterbalance the evolution of the spectrum along the tank, an existing wave generation procedure iterates on the wavemaker motions until the measured spectrum at X_t lies on $S_{\text{design}}(f)$ [4], [5]. It allows for the accurate generation of a unidirectional design spectrum at any position in the tank.

This procedure was successfully tested experimentally in [17] with a non breaking sea state. However, it was found that, for a same qualified the spectrum, the crest height distribution vary depending on X_t. It is important to understand that the crest distribution is a crucial quantity. It directly characterizes the severity of the most extreme events occurring at P_{design}. Therefore, the variation of the crest distribution depending on X_t questions the relevance of the procedure.

The objective of the present study is to test experimentally the procedure for an extreme breaking sea state. We do not study here the influence of X_t. We want to check the ability of the procedure to reproduce the same extreme sea state, without varying X_t, at different generation scales, in different wave tanks.

The first section of the paper describes the spectrum correction procedure. The second section details the experimental set-ups and the wave conditions. The third section presents the spectrum at X_t for all the generated configuration. And the last section compares the wave statistics.

II. Wave Generation procedure

This section gives a brief overview of the wave generation procedure used. It allows for the accurate control of the wave spectrum at any target position X_t in the tank.

A. Irregular wave generation

To generate a design sea state, several realizations are run. Each rely on a free surface elevation sequence $\eta_{\text{input}}(t)$ (t the time) used as input for the wavemaker. $\eta_{\text{input}}(t)$ is defined through a set of input Fourier amplitude $A_{\text{input}}(f)$ and random phases $\varphi_{\text{input}}(f)$. It is expressed as

$$\eta_{\text{input}}(t) = \sum_j A_{\text{input}}(f_j) \exp\left(i(2\pi f_j t + \varphi_{\text{input}}(f_j))\right) \quad (1)$$

The corresponding wavemaker motion is obtained using a linear transfer function that depends only of the wavemaker geometry.

B. Control of the spectrum at $x = X_t$

The wave qualification criteria impose that the measured wave spectrum at $x = X_t$, $S(f, X_t)$ (x the distance from the wavemaker) lies on the design spectrum $S_{\text{design}}(f)$.

Within the framewotk of linear dispersive wave theory, $A_{\text{input}}(f) = A_{\text{design}}(f)$ lead to the design spectrum at X_t. However, as mentioned in the Introduction, the wave propagation is not linear. Breaking events and nonlinear interactions affect the shape of the spectrum.

To counter balance those effect, the wave generation procedure used for the present study iterates on the input fourier amplitudes $A_{\text{input}}(f)$. At first, the realizations are generated using $A^0_{\text{input}}(f) = A_{\text{design}}(f)$ (iteration 0). Then, the input Fourier amplitudes are corrected depending on the measured amplitudes at $x = X_t$, $A^0(f, X_t)$. For iteration 1,

$$A^1_{\text{input}}(f) = A^0_{\text{input}}(f).A_{\text{design}}(f)/A^0(f, X_t) \quad (2)$$

The process is repeated iteratively until $S(f, X_t)$ reached S_{design}. The qualification of $S(f, X_t)$ relies on the maximum relative error E_{max} over the frequencies $f \in [0.75f_p, 1.25f_p]$ (f_p being the peak frequency of S_{design})

$$E_{max} = \text{Max}((S_{\text{design}}(f) - S(f, X_t))/S_{\text{design}}(f)) \quad (3)$$

More details about the procedure can be found in [4], [17].

III. Experimental set-up

The objective of the present study was to reproduce an extreme sea state at several scales in different experimental wave tanks. This section summarized the experimental set-ups adopted. The wave condition are also detailed.

A. Wave Conditions

TABLE I
Characteristics Of The Generated Sea State

	full scale	**scale 50**	**scale 94**
H_s	17.0m	0.340m	0.180m
T_p	15.5s	2.20s	1.60s
λ_p	375m	7.50m	4.00m
γ	2.6	2.6	2.6
$\epsilon = H_s/\lambda_p$	4.5%	4.5%	4.5%
ν_w	0.202	0.202	0.202

The characteristics of the wave conditions are gathered in Table I. λ_p refers to the peak wavelength, γ to the peak enhancement factor and ν_w to the non-dimensional spectral width (see [17], [18] for its definition). The sea state is a JONSWAP spectrum. The definition of the shape can be found in [19]. The steepness is large, $\epsilon = H_s/\lambda_p = 4.5\%$. It corresponds to an extreme wave condition, associated with strong breaking events. Note that this sea state was numerically studied in [4] and [5].

Two generation scales were adopted, 50 and 94. Scaling was performed using the Froud similitude. This is well adapted to the ocean wave propagation as it allows to keep constant the steepness and the relative depth. However, the strongly breaking wave condition studied here might lead to different behaviour depending on the scale, as breaking is beyond the framework of deep water depth dispersive waves theory.

B. Configurations studied

The experiments were performed in two tanks of the Ecole Centrale de Nantes (ECN) facilities, the Towing tank and the Ocean engineering wave tank. For seek of brevity, they will now be mentioned as T. tank and O.E. tank respectively. Their characteristics are detailed in Table II. More details can be found in the ECN website[1]. Three configuration were

[1]https://lheea.ec-nantes.fr/english-version/test-facilities/ocean-tanks

TABLE II
CHARACTERISTICS OF THE WAVE TANKS

	O.E. tank	**T. tank**
length	50m	150m
width	30m	5m
depth	5m	2.9m
Wave maker type	flap	flap
Hinge depth (from bottom)	2.15m	0.47m

explored: i) O.E tank scale 50 , ii) O.E. tank scale 94 and iii) T. tank scale 94. For each case, the target location was fixed to $X_t = 2\lambda_p$. Resistive wave gauges were set along the domains. For technical issue, the probe measurement network differed from one configuration to an other. But a probe was always set at $x = X_t$.

IV. CONTROLLED GENERATION OF THE TARGET SPECTRUM

We now present the results of the study. The procedure previously described was applied to generate the design sea state at $X_t = 2\lambda_p$ i) in i O.E tank at scale 50 , ii) in O.E. tank at scale 94 and iii) in T. tank at scale 94. This section is dedicated to the control of the spectrum at the target location for all the configurations.

A. Iterative correction

First, we detail the iterative correction of the spectrum at $x = X_t$. For the seek of brevity we illustrate the procedure with the scale 94 in the O.E. tank. Note that similar results were obtained for the other configurations.

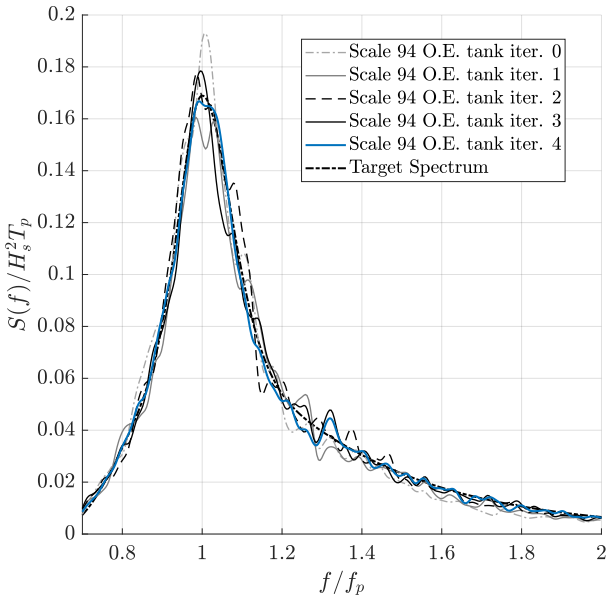

Fig. 1. O.E. tank scale 94. Iterative correction of the measured spectrum at $x = X_t$.

TABLE III
O.E. TANK SCALE 94, SPECTRUM PARAMETERS AT $x = X_t$, ITERATIONS 0 TO 4

	Iter. 0	**Iter. 1**	**Iter. 2**	**Iter. 3**	**Iter. 4**
$H_s/H_{s_{\text{design}}}$ (%)	99	98	100	99	99
$T_p/T_{p_{\text{design}}}$ (%)	99	102	101	100	101
ν_w	0.184	0.197	0.192	0.201	0.199
$E_{\max}$ (%)	24	32	32	13	15

Table III and Figure IV-A respectively give the characteristics and the shape of the spectrum at $x = X_t$ for all the iterations of the correction procedure.

Without any correction (iteration 0), the spectrum did not lie on its design shape. The peak was too high, the width too small and the maximum relative error reached 24%. Note that for an experimental configuration, the spectrum is considered as qualified if $E_{\max} < 10\%$ (see [17]). For the present study, dealing with an extreme sea state, the tolerance was raised up to 15%.

It is important to discriminate here three phenomena. First, breaking events occurred. It dissipated energy in the high frequency domain. This explained the small width and the too low spectrum tail. However, the measured H_s at X_t equaled 99% of the target H_s, even if breaking clearly dissipated energy. This means that either (i) the spectrum generated at $x = 0$ was too energetic (wave maker transfer function uncertainty) or (ii) the wave gauge overestimated the height of the waves (wave probe uncertainty). Note that (ii) can not affect the local shape of the spectrum. Wave gauge uncertainty only affect the magnitude of the wave spectrum (same relative error over all the frequency domain). The measurement uncertainty was estimated to 3%, using the methods described in [17].

Then the iterative correction process corrected the spectrum at $x = X_t$. Note that the process was not straightforward. As an example, the peak of the measured spectrum consecutively overshot or undershot its target value from one iteration to an other. The linear correction (Eqs 2) did not directly correct the spectrum shape. This means that the phenomena at the origin of the spectrum deviations were not linear.

Finally, At iteration 4, the spectrum almost lied on $S_{\text{design}}(f)$. E_{max} decreased to 15%. The spectrum was qualified at $x = X_t$. Similar results were obtained for the other configurations studied.

B. Controlled spectrum at X_t

TABLE IV
SPECTRUM PARAMETER AT $x = X_t$ AFTER CORRECTION

	O.E. scale 50	**O.E. scale 94**	**Towing scale 94**
$H_s/H_{s_{\text{design}}}$ (%)	99	99	96
$T_p/T_{p_{\text{design}}}$ (%)	98	101	99
ν_w	0.191	0.199	0.184
$E_{\max}$ (%)	15	15	11

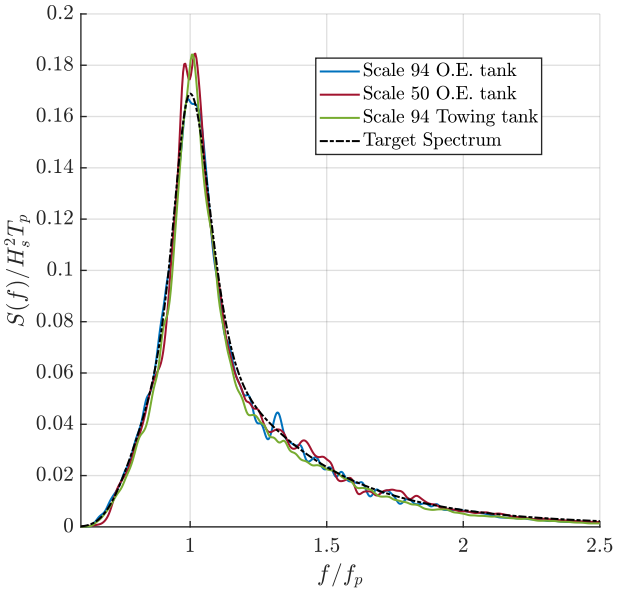

Fig. 2. Spectrum at $x = X_t$ after the correction procedure.

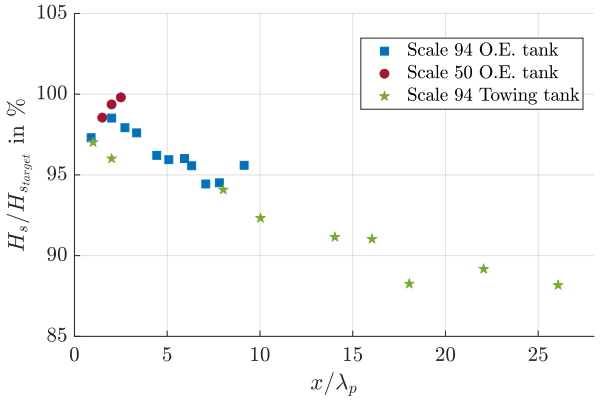

Fig. 3. H_s along the tank after correction of the spectrum at $x = X_t$.

We now present the spectrum obtained at $x = X_t$ after correction for O.E. tank scale 50, O.E. tank scale 94 and T. tank scale 94. The results are gathered in Table IV-B (spectrum parameters) and Figure IV-B (spectrum shape).

The error E_{max} was decreased to 15%, 15% and 11% for O.E. scale 50, O.E. scale 94 and T. scale 94 respectively. The spectrum at $x = X_t$ was qualified for all the configurations. Note that for O.E. scale 50 and T. scale 94 the peak was slightly overshot. As it will be seen in the next section, this might not affect the statistical behaviour of the wave field. The statistical quantities were not correlated with the variations of the spectrum depending on the configuration.

Complementary, Figure IV-B shows the evolution of the significant wave height along the tank (after correction of the spectrum at $x = X_t$). The trend is similar for O.E. scale 94 and T. scale 94 configurations (for O.E. scale 50 the number of probe is not sufficient to discriminate any spatial evolution). Independently of the tank, H_s decreased along the domain, due to breaking dissipation. The slope does not significantly changed from one configuration to an other. Note that some random variations affected the results. They were likely to be a consequence of the measurement uncertainty. Near the target location, H_s stayed around its target value. This was ensured by the spectrum correction procedures.

The procedure allowed for the accurate reproduction of the extreme design spectrum in the two tanks at the two significantly different generation scales.

V. Comparison of the wave statistics

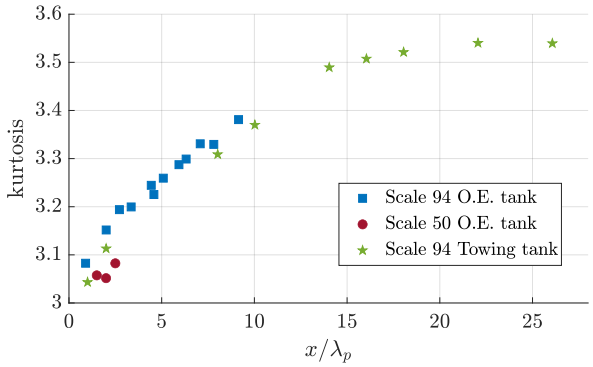

Fig. 4. Kurtosis along the tank after correction of the spectrum at $x = X_t$.

We will now focus on the statistical properties of the generated wave fields. First Figure V presents the evolution of the kurtosis of the free surface elevation η along the tank. This quantity is defined as the fourth moment of the η distribution. It is mainly used by the Ocean Engineering and the coastal engineering community to characterise the severity of a wave field [10], [20]. A large kurtosis is related to a large probability of occurrence of the extreme events.

For a linear wave field, the statistics are Gaussian (i. e. the shape of the probability density function is a Gaussian). The kurtosis is then equal to 3. Note that the wavemaker input sequences η_{input} were Gaussian (as a linear sum of independent frequency components).

In Figure V, for the three studied configurations, the kurtosis was larger than 3 from the beginning of the domain and increased with the distance from the wavemaker. Two phenomena should be discriminated. First, bound waves affected the shape of the wave fields making the crests higher, slightly increasing the kurtosis. The magnitude of the effect was constant all along the domain. Then the high order nonlinear interactions (mentioned in the Introduction) increased the occurrence of the extreme events along the tank.

Some differences can be observed while comparing the three generated configurations. The scale influenced the kurtosis at the target location. The O.E. scale 50 kurtosis values around $x = X_t$ are smaller than the one measured for O.E. scale 94 and T. scale 94 configurations. Note that at scale 94, independently of the tank, the kurtosis evolution was almost identical.

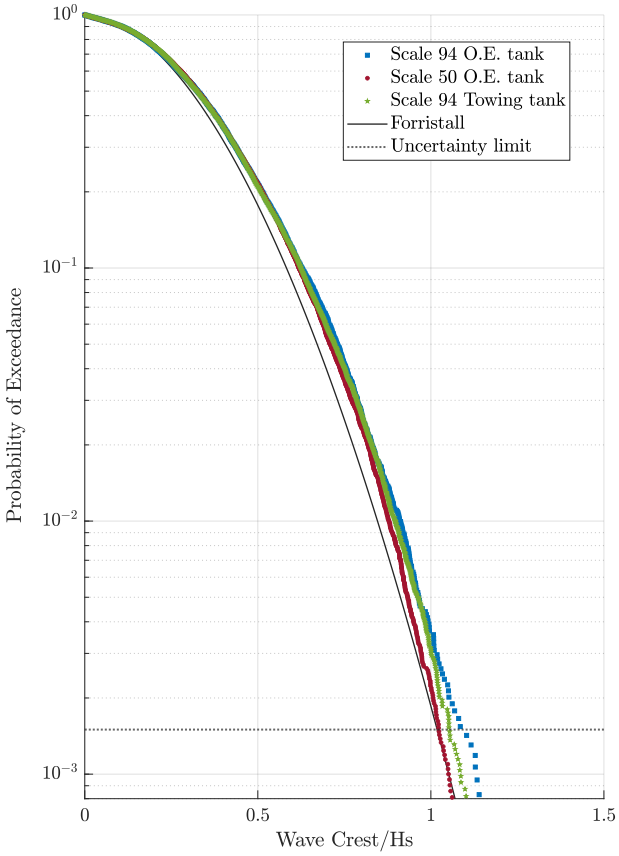

Fig. 5. Crest distribution at $x = X_t$ after after correction of the spectrum.

Figure V presents the crest distributions obtained at $x = X_t$. The results should be related to the kurtosis values measured at $x = X_t$. Note that the distributions are not statistically reliable for the probabilities below $1.5\ .10^{-3}$ (see the uncertainty limit line in Figure V). This has been estimated through the use of Jeffrey intervals, not displayed here for the seek of brevity (the method is described in [4], [17]). Note that $1.5\ .10^{-3}$ corresponds to a typical design probability P_{design} (see the Introduction of the present paper). The semi empirical Forristal reference is displayed. This distribution was built accounting for the second order effects, including the bound waves [21]). The ocean engineering community usually uses it as a benchmark [1], [3].

For probabilities above 10^{-2} independently of the studied configuration, the height of the crests were similar, larger than the one predicted by the Foristall reference. However, for probabilities below 10^{-2} the experimental results varied from one configuration to an other. The distribution measured for O.E. scale 50 lied on the Forristall reference but at scale 94, the events were more extreme. The influence of the tank (obtained when comparing T. scale 94 and O.E. scale 94) was almost non existent. However depending on the scale, the same qualified spectrum led to different statistical behaviours. Breaking was likely to be at the origin of the scale effect. The obtained results tended to demonstrate that smaller generation scales (i. e. larger waves) lead to more extreme events at a same probability level. More accurate studied should be performed to validate, quantify and explain the phenomenon.

VI. Conclusion

An extreme breaking sea state was reproduced in two tanks at two different generation scales. An iterative correction procedure was used to ensure the quality of the wave spectrum at the same relative distance from the wave maker $X_t = 2\lambda_p$. The spectrum was accurately reproduced at X_t for all the studied cases. Due to the complex and extreme nonlinear phenomena affecting the propagation of the waves, small deviations of the spectra from their shape could still be observed after the correction procedures. However, the maximum relative error $E\max$ remained below 15%.

The crest distribution at the target location was not significantly influenced by the domain (i.e. wave tank and wave maker transfer function). This means that the spectrum correction procedure can reproduce a same statistical behaviour in several experimental facilities (if using the same target location X_t). However, the statistics varied depending on the generation scale. Note that the variations were uncorrelated to the observed spectrum variations. It seems that the characteristics of the breaking events were influenced by the scale. A smaller scale (larger waves) led to more extreme events. More detailed investigation should be carry out to quantify this effect. The crest distribution is a crucial quantity for wave structure interaction tests. The wave generation and qualification practices should then consider the influence of the generation scale when studying breaking sea states.

Acknowledgment

This work was performed in the framework of the Chaire Hydrodynamique et Structure Marines CENTRALE NANTES - BUREAU VERITAS. The experimental study was inspired by the currently running Joint Industry Project (JIP) 'Reproducible CFD Modeling Practice for Offshore Applications'.

References

[1] Det Norske Veritas, "Environmental conditions and environmental loads, recommended practice dnv-rp-c205," 2010.

[2] V. E. Zakharov, V. S. L'vov, and G. Falkovich, *Kolmogorov spectra of turbulence I: Wave turbulence*. Springer Science & Business Media, 2012.

[3] NWT Preparation Workgroup, "Year 1 report," JIP on Reproducible CFD Modeling Practice for Offshore Applications, Tech. Rep., 2019.

[4] M. Canard, G. Ducrozet, and B. Bouscasse, "Generation of 3hr long-crested waves of extreme sea states with hos-nwt solver," in *ASME 2020 39th International Conference on Ocean, Offshore and Arctic Engineering*. American Society of Mechanical Engineers Digital Collection, 2020.

[5] S. Fouques, C. Eloïse, H.-J. Lim, J. Kim, M. Canard, G. Ducrozet, B. Bouscasse, A. Koop, B. Zhao, W. Wang, and H. Bihs, "Qualification criteria for the verification of numerical waves - part 1: Potential-based numerical wave tank (pnwt)," in *ASME 2021 40th International Conference on Ocean, Offshore and Arctic Engineering*. American Society of Mechanical Engineers Digital Collection, 2021.

[6] S. Y. Annenkov and V. I. Shrira, "Role of non-resonant interactions in the evolution of nonlinear random water wave fields," *Journal of Fluid Mechanics*, vol. 561, pp. 181–207, 2006.
[7] P. A. Janssen, "Nonlinear four-wave interactions and freak waves," *Journal of Physical Oceanography*, vol. 33, no. 4, pp. 863–884, 2003.
[8] F. Fedele, "On the kurtosis of deep-water gravity waves," *Journal of Fluid Mechanics*, vol. 782, pp. 25–36, 2015.
[9] M. Onorato, A. R. Osborne, M. Serio, L. Cavaleri, C. Brandini, and C. Stansberg, "Extreme waves, modulational instability and second order theory: wave flume experiments on irregular waves," *European Journal of Mechanics-B/Fluids*, vol. 25, no. 5, pp. 586–601, 2006.
[10] M. Onorato, L. Cavaleri, S. Fouques, O. Gramstad, P. A. Janssen, J. Monbaliu, A. R. Osborne, C. Pakozdi, M. Serio, C. Stansberg *et al.*, "Statistical properties of mechanically generated surface gravity waves: a laboratory experiment in a three-dimensional wave basin," *Journal of Fluid Mechanics*, vol. 627, pp. 235–257, 2009.
[11] L. Shemer, A. Sergeeva, and D. Liberzon, "Effect of the initial spectrum on the spatial evolution of statistics of unidirectional nonlinear random waves," *Journal of Geophysical Research: Oceans*, vol. 115, no. C12, 2010.
[12] Z. Cherneva, M. Tayfun, and C. Guedes Soares, "Statistics of nonlinear waves generated in an offshore wave basin," *Journal of Geophysical Research: Oceans*, vol. 114, no. C8, 2009.
[13] G. Michel, F. Bonnefoy, G. Ducrozet, G. Prabhudesai, A. Cazaubiel, F. Copie, A. Tikan, P. Suret, S. Randoux, and E. Falcon, "Emergence of peregrine solitons in integrable turbulence of deep water gravity waves," *Physical Review Fluids*, vol. 5, no. 8, p. 082801, 2020.
[14] T. Tang, W. Xu, D. Barratt, H. B. Bingham, Y. Li, P. Taylor, T. Van Den Bremer, and T. Adcock, "Spatial evolution of the kurtosis of steep unidirectional random waves," *Journal of Fluid Mechanics*, vol. 908, 2021.
[15] M. Latheef and C. Swan, "A laboratory study of wave crest statistics and the role of directional spreading," *Proceedings of the Royal Society A: Mathematical, Physical and Engineering Sciences*, vol. 469, no. 2152, p. 20120696, 2013.
[16] Q. Derbanne, O. Menard, M. Darquier, and D. Frechou, "Génération, propagation et dissipation de la houle en bassin d'essai de très grande longueur," in *Proc. of ATMA 2019*, 2009.
[17] M. Canard, G. Ducrozet, and B. Bouscasse, "Varying ocean wave statistics emerging from a single energy spectrum in an experimental wave tank," *Ocean Engineering*, 2022 (acceptedfor publication).
[18] M. Serio, M. Onorato, A. R. Osborne, P. Janssen *et al.*, "On the computation of the benjamin-feir index," 2005.
[19] G. J. Komen, L. Cavaleri, M. Donelan, K. Hasselmann, S. Hasselmann, and P. Janssen, "Dynamics and modelling of ocean waves," *Dynamics and Modelling of Ocean Waves, by GJ Komen and L. Cavaleri and M. Donelan and K. Hasselmann and S. Hasselmann and PAEM Janssen, pp. 554. ISBN 0521577810. Cambridge, UK: Cambridge University Press, August 1996.*, p. 554, 1996.
[20] M. Christou and K. Ewans, "Field measurements of rogue water waves," *Journal of physical oceanography*, vol. 44, no. 9, pp. 2317–2335, 2014.
[21] G. Z. Forristall, "Wave crest distributions: Observations and second-order theory," *Journal of physical oceanography*, vol. 30, no. 8, pp. 1931–1943, 2000.